PHYSICAL REVIEW B **107**, L041405 (2023)

Letter

Nonlinear circular dichroism in achiral dielectric nanoparticles

Anastasia Nikitina,* Anna Nikolaeva, and Kristina Frizyuk†
The Faculty of Physics, ITMO University, Saint Petersburg, Russia, 197101

(Received 10 August 2022; revised 2 January 2023; accepted 9 January 2023; published 20 January 2023)

We present a theoretical study of *circular dichroism* in the *second-harmonic* signal of single dielectric nanostructures with different symmetries and noncentrosymmetric materials. We show that this effect is defined not only by macroscopic (particle) and lattice symmetries but also by their relative orientation. Using symmetry and modal analysis, we provide a general and very simple formula to determine whether the dichroism exists and a chart with the most significant cases.

DOI: 10.1103/PhysRevB.107.L041405

Introduction. Chirality is a property that plays a significant role in physics, chemistry, biology, and medicine. Many examples of chirality can be found in nature, for example, in amino acids, which often have inherent handedness [1,2]. *Circular dichroism spectroscopy* is an excellent method for evaluating the unique properties of proteins, molecules, and chiral materials [3–6]. As chiral effects are usually weakly manifested in natural media, chiral metamaterials [7–9] and chiral plasmonic structures [10–14], for example, with Fano-enhanced circular dichrosim (CD) [15,16], have been widely used in recent years as a useful tool for achieving strong chiroptical responses.

Circular dichroism can be obtained in nonlinear optical processes, such as second- and third-harmonic generation. Circularly polarized light interacting with resonances of nanostructures in the nonlinear regime can produce a significant chiroptical signal, which is of great interest due to its high sensitivity to symmetry breaking [17–21]. Generally, this nonlinear effect is observed in chiral plasmonic structures, for example, G-shaped structures [22–24], structures with C_n rotational symmetry [9,25,26], or structures with other chiral asymmetric shapes [27–30]. Meanwhile, the crystalline lattices of dielectric nanostructures with a huge second-order susceptibility have no inversion symmetry [31–34], which makes them promising for circular dichroism spectroscopy. Owing to the presence of Mie resonances [35,36], anapole states [37,38], and quasibound states in the continuum [29,39], such structures can generate locally enhanced electromagnetic fields needed for sensitive CD measurements. Researchers have already developed several approaches to enhancing chiroptical signals using nanoparticles [40–42]. Sometimes, objects that, at first glance, are not chiral demonstrate an unexpected chiroptical response. Such a response can be enabled by symmetry breaking at arbitrary incidence on the metasurface [43–48], "structural" effects (relative orientation of meta-atoms in an array) [49,50], or another nontrivial reason, such as different coupling to the multipole moments of the structure [51], rotation of the particles [52], asymmetric excitation [53], plasmonic enhancement of a small chiroptical response [54], or even an oriented intermediate state in single atoms [55]. Surprisingly, for the second harmonic (SH) in achiral nanostructures, strong nonlinear CD can also appear, as was shown in Ref. [56]. In this Research Letter, we provide a general rule for determining when nonlinear circular dichroism occurs in achiral dielectric nanoparticles: This fast and convenient method will save time for researchers in this rapidly developing field and could be particularly useful for chiral sensing [57–60]. Indeed, if a nanoparticle or nanostructure [61,62] is used to amplify the chiral signal, the chiral signal from the structure itself must be excluded. In addition, if the second harmonic demonstrates a strong dichroism, this will also affect the linear response, because a different amount of energy will be converted into the doubled-frequency mode.

Results. We analyze the possibility of observing SH-CD in achiral nanoparticles with different symmetries and materials. We consider the following geometry: A nanoparticle with a C_{nv} or D_{nh} symmetry (a pyramid or a prism with a regular polygon base [63]), with the symmetry axis along the z axis, is irradiated by a normally incident circularly polarized plane wave (LCP and RCP indicate left and right circular polarization, respectively); see Fig. 1. We assume that our nanoparticle is fabricated from a monocrystalline bulk sample using lithography. In this case, we can "cut out" this nanoparticle under different angles with respect to the lattice orientation. We fix the lattice orientation and suppose that the nanoparticle is rotated by an angle β with respect to the lattice axis, as shown in Fig. 1. The presence of a substrate does not alter the result. SH-CD is described by the following formula [64–66]:

$$\text{SH-CD} = 2\frac{\left(I_{\text{RCP}}^{2\omega} - I_{\text{LCP}}^{2\omega}\right)}{\left(I_{\text{RCP}}^{2\omega} + I_{\text{LCP}}^{2\omega}\right)}, \tag{1}$$

where $I_{\text{RCP}}^{2\omega}$ and $I_{\text{LCP}}^{2\omega}$ are the total second-harmonic intensity integrated over all the angles for incident RCP and LCP waves, respectively. If these intensities are different, we can say that nonlinear circular dichroism appears.

The main results are presented in Fig. 2. In the leftmost column, different particle symmetries (with examples of

---

*anastasia.nikitina@metalab.ifmo.ru

†k.frizyuk@metalab.ifmo.ru

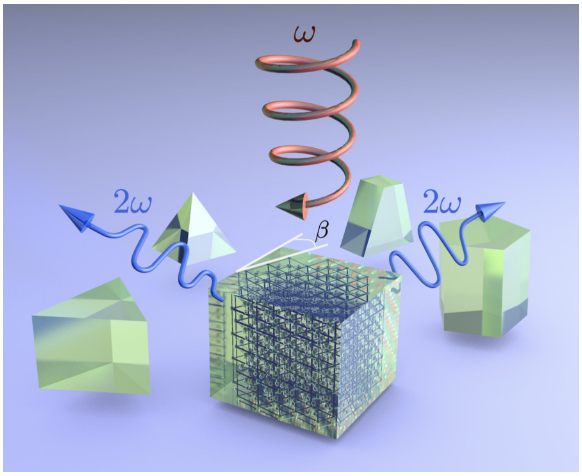

FIG. 1. Schematic of the concept. A single symmetric nanoparticle (for example, a cube, prism, or pyramid) with a certain lattice symmetry and orientation generates a second harmonic when excited by a circularly polarized wave. β is the angle between a certain vector of the crystalline lattice and a chosen axis of the nanoparticle. Examples of different nanoparticles are shown.

corresponding particle shapes) are shown. Let us note that the exact shape does not affect the results. For example, we can consider a trimer structure in the same way as a triangular prism if they both possess D_{3h} symmetry. The incident wavelength does not play a major role either, but for a more pronounced SH-CD, we chose it to be in the vicinity of the first Mie resonances. In the leftmost column, we show some relative angles β between the lattice axis/vector and nanoparticle axis for a fixed lattice position, as shown in the uppermost row. Our method is applicable for any crystalline lattice orientation if the initial (not rotated) nonlinear susceptibility tensor $\hat{\chi}^{(2)}$ is known. The "rotated" tensor for different orientations [67] is obtained with the MATLAB code given in the Supplemental Material [68]. In our considerations, we assume that all the fields are decomposed into a series of multipoles [69,70], but we will be interested only in the total angular momentum projection m. In the uppermost row, we also provide the SH power flow into the upper half- space with an angular distribution for a single cylindrical or conical particle. Such patterns with several petals can be formed only if the radiation has several different angular momentum projections m. The number of petals depends on the difference between the projections.

In Fig. 2 we put a check mark if the dichroism appears. It usually exists for all angles β except for a finite number of angles, which are also given in each cell. We put a cross if SH-CD never appears for such a particle shape and orientation.

Theory. Although the theory of second-harmonic generation in nanostructures has already been sufficiently developed in previous works [56,70], manually considering each individual case is time-consuming and requires lengthy calculations. Moreover, both at the first- and the second-harmonic frequencies, several modes of different symmetry are excited, and all of them must be considered differently, depending on whether they are degenerate or not. However, we propose a simple approach based on the law of conservation of momentum projection [70,71]. It consists of several simple steps (which are given in detail in the Supplemental Material [68] (see also Refs. [72–77] therein)).

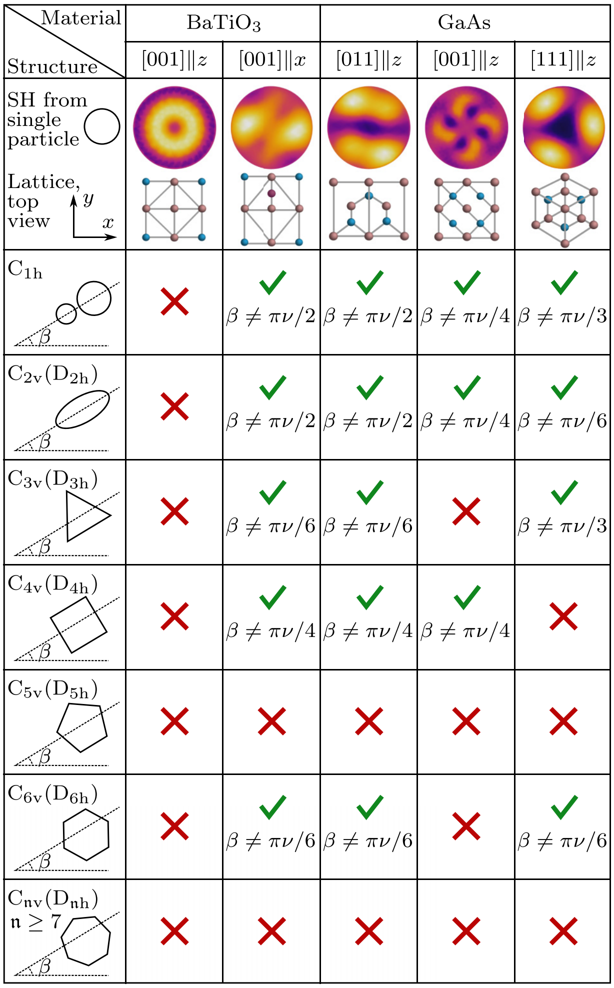

Structure \ Material	BaTiO$_3$		GaAs		
	$[001]\|z$	$[001]\|x$	$[011]\|z$	$[001]\|z$	$[111]\|z$
SH from single particle Lattice, top view y x					
C_{1h}	✗	✓ $\beta \neq \pi\nu/2$	✓ $\beta \neq \pi\nu/2$	✓ $\beta \neq \pi\nu/4$	✓ $\beta \neq \pi\nu/3$
$C_{2v}(D_{2h})$	✗	✓ $\beta \neq \pi\nu/2$	✓ $\beta \neq \pi\nu/2$	✓ $\beta \neq \pi\nu/4$	✓ $\beta \neq \pi\nu/6$
$C_{3v}(D_{3h})$	✗	✓ $\beta \neq \pi\nu/6$	✓ $\beta \neq \pi\nu/6$	✗	✓ $\beta \neq \pi\nu/3$
$C_{4v}(D_{4h})$	✗	✓ $\beta \neq \pi\nu/4$	✓ $\beta \neq \pi\nu/4$	✓ $\beta \neq \pi\nu/4$	✗
$C_{5v}(D_{5h})$	✗	✗	✗	✗	✗
$C_{6v}(D_{6h})$	✗	✓ $\beta \neq \pi\nu/6$	✓ $\beta \neq \pi\nu/6$	✗	✓ $\beta \neq \pi\nu/6$
$C_{\mathfrak{n}v}(D_{\mathfrak{n}h})$ $\mathfrak{n} \geq 7$	✗	✗	✗	✗	✗

FIG. 2. Main results regarding the existence of nonlinear circular dichroism in achiral nanoparticles with different symmetries and crystalline lattices. The uppermost row shows the angular dependence of the SH power flow into the upper half-space for a single cylindrical or conical particle for each crystalline lattice, and the top view of the lattices. Below this row, we provide the analysis results for different symmetry groups: Either SH-CD appears for all particle rotation angles β, except for certain angles, or it is not possible at all.

(1) The incident LCP or RCP plane wave has a projection $m^{\text{wave}} = \pm 1$. Thus it excites the modes in the nanoparticle.

(2) If the nanoparticle has $\mathfrak{n}$-fold rotational symmetry, an additional momentum exists, which is a multiple of $\mathfrak{n}$. Thus, at the fundamental frequency, modes containing terms with the following m values are excited inside the nanoparticle: $m^{\text{in}} = \pm 1 + \mathfrak{n}\nu$, $\nu \in \mathbb{Z}$.

(3) The nonlinear polarization is written as follows: $\mathbf{P}^{2\omega}(\mathbf{r}) = \varepsilon_0 \hat{\chi}^{(2)} \mathbf{E}^{\text{in}}(\mathbf{r}) \mathbf{E}^{\text{in}}(\mathbf{r})$, where the field inside the nanostructure $\mathbf{E}^{\text{in}}(\mathbf{r})$ has the momentum m^{in}, and the additional momentum m_χ is created due to the lattice symmetry. This expression can be easily obtained by rewriting the tensor in cylindrical coordinates [78].

(4) Combining all the additional terms, we obtain that modes with $m^{2\omega} = \pm 2 + \mathfrak{n}\nu + m_\chi$ are excited at the doubled frequency with the additional phase $-m_\chi \beta$, which is also seen from the tensor in cylindrical coordinates.

(5) We should note that there are always several different m_χ. We introduce Δm_χ as the difference between any two values of m_χ.

(6) Then, we consider the excitation of two modes with the difference Δm_χ. For LCP, the polarization will be proportional to

$$\mathbf{P}^{2\omega}(\mathbf{r}) \propto \sum_\nu e^{-im_\chi\beta}\big[\mathbf{P}^{2\omega}_{m^{2\omega},\nu}(r,z)e^{i\varphi(2+\mathfrak{n}\nu+m_\chi)} + \mathbf{P}^{2\omega}_{m^{2\omega}+\Delta m_\chi,\nu}(r,z)e^{i\varphi(2+\mathfrak{n}\nu+m_\chi+\Delta m_\chi)}e^{-i\Delta m_\chi\beta}\big]. \quad (2)$$

For RCP, we consider the modes with opposite $m^{2\omega}$; due to the tensor structure, they are always presented

$$\mathbf{P}^{2\omega}(\mathbf{r}) \propto \sum_\nu e^{im_\chi\beta}\big[\mathbf{P}^{2\omega}_{-m^{2\omega},\nu}(r,z)e^{i\varphi(-2+\mathfrak{n}\nu-m_\chi)} + \mathbf{P}^{2\omega}_{-m^{2\omega}-\Delta m_\chi,\nu}(r,z)e^{i\varphi(-2+\mathfrak{n}\nu-m_\chi-\Delta m_\chi)}e^{i\Delta m_\chi\beta}\big]. \quad (3)$$

(7) Now, we recall that the structure is not chiral; thus modes with opposite $m^{2\omega}$ are excited by the same polarization terms $[|P^{2\omega}_{m^{2\omega},\nu}(r,z)| = |P^{2\omega}_{-m^{2\omega},\nu}(r,z)|]$ with the same weight. However, the phase difference between modes, $e^{i\Delta m_\chi\beta}$, is different for LCP and RCP cases, which means that if these modes interfere, they will interfere differently for two incident wave polarizations. Thus, in order for the SH-CD to appear, we need these modes to interfere, and $e^{i\Delta m_\chi\beta} \neq e^{-i\Delta m_\chi\beta}$.

Summarizing the above considerations, we derived a rule that is applicable for all cases of SH-CD in achiral structures. All we need to know is the susceptibility tensor $\hat{\chi}^{(2)}$ in cylindrical coordinates and the symmetry group $\mathrm{C}_{\mathfrak{n}\mathrm{v}}(\mathrm{D}_{\mathfrak{n}\mathrm{h}})$ of the considered nanoparticle. The tensor $\hat{\chi}^{(2)}$ in cylindrical coordinates contains exponential terms, $e^{im_\chi\varphi}$, and therefore we introduce Δm_χ as the difference between any two m_χ. For several lattices, we present all the possible Δm_χ in the headings at the top of Fig. 3. After that, one can find the angles β of the crystalline lattice rotation at which nonlinear circular dichroism appears.

Main rule. If there is a number $\nu \in \mathbb{Z}$ such that the difference between the angular momentum projections Δm_χ from the nonlinear susceptibility tensor is equal to $\nu\mathfrak{n}$, where $\mathfrak{n}$ is related to the symmetry group, we introduce the number s:

$$s = \Delta m_\chi = \nu\mathfrak{n}. \quad (4)$$

The nonlinear circular dichroism in such a nanoparticle appears for any angles of the crystalline lattice rotation

$$\beta \neq \frac{\pi\nu}{s}. \quad (5)$$

If such an integer number $\nu \in \mathbb{Z}$ exists for several Δm_χ, then it is necessary to choose only those angles $\beta \neq \pi\nu/s$ that are the same for all $s = \Delta m_\chi$.

Discussion. In short, CD is present when the modes excited by different terms of the $\hat{\chi}^{(2)}$ tensor have the same symmetry and interfere, and the phases depend on the incident polarization. This is possible only if (5) is satisfied. The application of the rule is shown in Fig. 3. We did not include the trivial case of the crystalline lattice $\mathrm{BaTiO_3}$ with [001]$\|z$. For this case, we only have single $m_\chi = 0$. Therefore circular dichroism in such a crystalline lattice is not possible for any symmetry of the nanoparticle, as nothing depends on the incident polarization. In this Research Letter, we omit the discussion of SH-CD strength for every particular case; huge values close to 1 have been achieved already [56], and an example is given in the Supplemental Material. However, we should note that SH-CD will have local maxima close to the resonances of the modes with $m^{2\omega} + \Delta m_\chi$, where the phases are changing rapidly, allowing constructive or destructive interference.

$\mathfrak{n}$	$\mathrm{GaAs}[001]\|z$ $\Delta m_\chi = 4$	$\mathrm{BaTiO_3}[001]\|x/$ $\mathrm{GaAs}[011]\|z$ $\Delta m_\chi = 2,4,6$	$\mathrm{GaAs}[111]\|z$ $\Delta m_\chi = 3,6$
1	$4 = 1\nu \rightarrow$ $s = 4$ $\beta \neq \pi\nu/4$	$2,4,6 = 1\nu \rightarrow$ $s = 2,4,6$ $\beta \neq \pi\nu/2$	$3,6 = 1\nu \rightarrow$ $s = 3,6$ $\beta \neq \pi\nu/3$
2	$4 = 2\nu \rightarrow$ $s = 4$ $\beta \neq \pi\nu/4$	$2,4,6 = 2\nu \rightarrow$ $s = 2,4,6$ $\beta \neq \pi\nu/2$	$3,6 = 2\nu \rightarrow$ $s = 6$ $\beta \neq \pi\nu/6$
3	$4 = 3\nu \rightarrow$ – *no*	$2,4,6 = 3\nu \rightarrow$ $s = 6$ $\beta \neq \pi\nu/6$	$3,6 = 3\nu \rightarrow$ $s = 3,6$ $\beta \neq \pi\nu/3$
4	$4 = 4\nu \rightarrow$ $s = 4$ $\beta \neq \pi\nu/4$	$2,4,6 = 4\nu \rightarrow$ $s = 4$ $\beta \neq \pi\nu/4$	$3,6 = 4\nu \rightarrow$ – *no*
5	$4 = 5\nu \rightarrow$ – *no*	$2,4,6 = 5\nu \rightarrow$ – *no*	$3,6 = 5\nu \rightarrow$ – *no*
6	$4 = 6\nu \rightarrow$ – *no*	$2,4,6 = 6\nu \rightarrow$ $s = 6$ $\beta \neq \pi\nu/6$	$3,6 = 6\nu \rightarrow$ $s = 6$ $\beta \neq \pi\nu/6$
≥ 7	$4 = \mathfrak{n}\nu \rightarrow$ – *no*	$2,4,6 = \mathfrak{n}\nu \rightarrow$ – *no*	$3,6 = \mathfrak{n}\nu \rightarrow$ – *no*

FIG. 3. Illustration of the main rule for different cases. For each crystalline lattice and symmetry group $\mathrm{C}_{\mathfrak{n}\mathrm{v}}(\mathrm{D}_{\mathfrak{n}\mathrm{h}})$, we show the number s and angles β at which nonlinear circular dichroism exists; "no" means that SH-CD is not possible. In the headings at the top, the difference Δm_χ between the angular momentum projections in the tensor $\hat{\chi}^{(2)}$ is also provided.

The correctness of the results was verified with the symmetry analysis of the overlap integrals (see Supplemental Material) and numerical modeling in COMSOL MULTIPHYSICS in the undepleted pump approximation. The method is well known, and it was described, for example, in Refs. [79,80].

Conclusion. In this Research Letter, we provide a simple rule based on angular momentum projection conservation and modal analysis: This rule allows us to determine when nonlinear circular dichroism appears for all possible shapes and crystalline lattices of an achiral $\mathrm{C}_{\mathfrak{n}\mathrm{v}}(\mathrm{D}_{\mathfrak{n}\mathrm{h}})$ nanoparticle. Moreover, the main formula does not depend on the angular momentum of the incident wave, which suggests that it could be applied for irradiation with beams of arbitrary angular momentum. The method can also provide ideas as to how to describe the appearance of CD in other systems where the lattice and meta-atom symmetries interact, for example, in metasurfaces with rotated meta-atoms. We can also assume that oblique wave incidence can be described as a normal incidence on a rotated particle, which can be equivalent to a particle of lower symmetry. A detailed study of these hypotheses may be the subject of further research.

Data and codes for the results presented in this Research Letter are available in the Supplemental Material [68] and Ref. [67].

Acknowledgments. The authors acknowledge Prof. Y. Kivshar for valuable advice and the initial impetus for this work; M. Glazov and other members of the Low-Dimensional Seminar at the Ioffe Institute; and M. Petrov, I. Toftul, K. Koshelev, and L. Pogorelskaya for many fruitful discussions. The numerical modelling was funded by RFBR and DFG according to the research Project No. 20-52-12062. Analytical calculations were supported by the Russian Science Foundation (Project No. 22-12-00204). The work was supported by the Priority 2030 Federal Academic Leadership Program. K.F. acknowledges support from the Foundation for the Advancement of Theoretical Physics and Mathematics "BASIS" (Russia).

---

[1] L. Pasteur, Ann. Chim. Phys. **xxiv**, 442 (1848).
[2] R. S. Cahn, C. Ingold, and V. Prelog, Angew. Chem., Int. Ed. Engl. **5**, 385 (1966).
[3] N. J. Greenfield, Nat. Protoc. **1**, 2876 (2006).
[4] B. Hopkins, A. N. Poddubny, A. E. Miroshnichenko, and Y. S. Kivshar, Laser Photonics Rev. **10**, 137 (2016).
[5] A. H. N. C. De Silva, D. Atri-Schuller, S. Dubey, B. P. Acharya, K. L. Romans, K. Foster, O. Russ, K. Compton, C. Rischbieter, N. Douguet, K. Bartschat, and D. Fischer, Phys. Rev. Lett. **126**, 023201 (2021).
[6] F. Graf, J. Feis, X. Garcia-Santiago, M. Wegener, C. Rockstuhl, and I. Fernandez-Corbaton, ACS Photonics **6**, 482 (2019).
[7] M. V. Gorkunov, A. A. Antonov, and Y. S. Kivshar, Phys. Rev. Lett. **125**, 093903 (2020).
[8] Y. Zhao, M. A. Belkin, and A. Alù, Nat. Commun. **3**, 870 (2012).
[9] D. Kim, J. Yu, I. Hwang, S. Park, F. Demmerle, G. Boehm, M.-C. Amann, M. A. Belkin, and J. Lee, Nano Lett. **20**, 8032 (2020).
[10] M. Schäferling, D. Dregely, M. Hentschel, and H. Giessen, Phys. Rev. X **2**, 031010 (2012).
[11] J. Li, M. Wang, Z. Wu, H. Li, G. Hu, T. Jiang, J. Guo, Y. Liu, K. Yao, Z. Chen, J. Fang, D. Fan, B. A. Korgel, A. Alù, and Y. Zheng, Nano Lett. **21**, 973 (2021).
[12] M. Hentschel, M. Schäferling, X. Duan, H. Giessen, and N. Liu, Sci. Adv. **3**, e1602735 (2017).
[13] J. T. Collins, C. Kuppe, D. C. Hooper, C. Sibilia, M. Centini, and V. K. Valev, Adv. Opt. Mater. **5**, 1700182 (2017).
[14] W. Chen, Q. Yang, Y. Chen, and W. Liu, Phys. Rev. Lett. **126**, 253901 (2021).
[15] A. V. Kondratov, M. V. Gorkunov, A. N. Darinskii, R. V. Gainutdinov, O. Y. Rogov, A. A. Ezhov, and V. V. Artemov, Phys. Rev. B **93**, 195418 (2016).
[16] Z. Liu, Y. Xu, C.-Y. Ji, S. Chen, X. Li, X. Zhang, Y. Yao, and J. Li, Adv. Mater. **32**, 1907077 (2020).
[17] T. Verbiest, M. Kauranen, A. Persoons, M. Ikonen, J. Kurkela, and H. Lemmetyinen, J. Am. Chem. Soc. **116**, 9203 (1994).
[18] K. Koshelev, Y. Tang, Z. Hu, I. Kravchenko, G. Li, and Y. Kivshar, ACS Photonics **10**, 298 (2023).
[19] M. A. Weissflog, M. Cai, M. Parry, M. Rahmani, L. Xu, D. Arslan, A. Fedotova, G. Marino, M. Lysevych, H. H. Tan, C. Jagadish, A. Miroshnichenko, G. Leo, A. A. Sukhorukov, F. Setzpfandt, T. Pertsch, I. Staude, and D. N. Neshev, Laser Photonics Rev. **16**, 2200183 (2022).
[20] A. Belardini, M. C. Larciprete, M. Centini, E. Fazio, C. Sibilia, D. Chiappe, C. Martella, A. Toma, M. Giordano, and F. Buatier de Mongeot, Phys. Rev. Lett. **107**, 257401 (2011).
[21] A. Belardini, G. Leahu, E. Petronijevic, T. Hakkarainen, E. Koivusalo, M. Rizzo Piton, S. Talmila, M. Guina, and C. Sibilia, Micromachines **11**, 225 (2020).
[22] V. K. Valev, A. V. Silhanek, N. Verellen, W. Gillijns, P. Van Dorpe, O. A. Aktsipetrov, G. A. E. Vandenbosch, V. V. Moshchalkov, and T. Verbiest, Phys. Rev. Lett. **104**, 127401 (2010).
[23] V. K. Valev, N. Smisdom, A. V. Silhanek, B. De Clercq, W. Gillijns, M. Ameloot, V. V. Moshchalkov, and T. Verbiest, Nano Lett. **9**, 3945 (2009).
[24] E. A. Mamonov, I. A. Kolmychek, S. Vandendriessche, M. Hojeij, Y. Ekinci, V. K. Valev, T. Verbiest, and T. V. Murzina, Phys. Rev. B **89**, 121113(R) (2014).
[25] K.-H. Kim and J.-R. Kim, Ann. Phys. (Berlin) **532**, 2000078 (2020).
[26] J. T. Collins, X. Zheng, N. V. S. Braz, E. Slenders, S. Zu, G. A. E. Vandenbosch, V. V. Moshchalkov, Z. Fang, M. Ameloot, P. A. Warburton, and V. K. Valev, Adv. Opt. Mater. **6**, 1800153 (2018).
[27] L. Kang, C.-Y. Wang, X. Guo, X. Ni, Z. Liu, and D. H. Werner, Nano Lett. **20**, 2047 (2020).
[28] R. Schreiber, N. Luong, Z. Fan, A. Kuzyk, P. C. Nickels, T. Zhang, D. M. Smith, B. Yurke, W. Kuang, A. O. Govorov, and T. Liedl, Nat. Commun. **4**, 2948 (2013).
[29] M. Gandolfi, A. Tognazzi, D. Rocco, C. De Angelis, and L. Carletti, Phys. Rev. A **104**, 023524 (2021).
[30] F. Spreyer, J. Mun, H. Kim, R. M. Kim, K. T. Nam, J. Rho, and T. Zentgraf, ACS Photonics **9**, 784 (2022).
[31] T. Liu, S. Xiao, B. Li, M. Gu, H. Luan, and X. Fang, Front. Nanotechnol. **4**, (2022).
[32] C. Gigli and G. Leo, Opto-Electron. Adv. **5**, 210093 (2022).
[33] D. Rocco, R. C. Morales, L. Xu, A. Zilli, V. Vinel, M. Finazzi, M. Celebrano, G. Leo, M. Rahmani, C. Jagadish, H. Tan, D. Neshev, and C. De Angelis, Adv. Phys.: X **7**, 2022992 (2022).
[34] L. Carletti, A. Locatelli, D. Neshev, and C. De Angelis, ACS Photonics **3**, 1500 (2016).
[35] D. Smirnova, A. I. Smirnov, and Y. S. Kivshar, Phys. Rev. A **97**, 013807 (2018).
[36] W. Chen, Q. Yang, Y. Chen, and W. Liu, ACS Omega **5**, 14157 (2020).
[37] E. Díaz-Escobar, T. Bauer, E. Pinilla-Cienfuegos, Á. I. Barreda, A. Griol, L. Kuipers, and A. Martínez, Light Sci. Appl. **10**, 204 (2021).
[38] H. Hu, Q. Gan, and Q. Zhan, Phys. Rev. B **105**, 245412 (2022).
[39] K. Koshelev and Y. Kivshar, ACS Photonics **8**, 102 (2021).
[40] S. Yoo and Q.-H. Park, Sci. Rep. **5**, 14463 (2015).

[41] D. Vestler, A. Ben-Moshe, and G. Markovich, J. Phys. Chem. C **123**, 5017 (2019).

[42] C.-S. Ho, A. Garcia-Etxarri, Y. Zhao, and J. Dionne, ACS Photonics **4**, 197 (2017).

[43] S. S. Kruk, A. N. Poddubny, D. A. Powell, C. Helgert, M. Decker, T. Pertsch, D. N. Neshev, and Y. S. Kivshar, Phys. Rev. B **91**, 195401 (2015).

[44] T. Verbiest, M. Kauranen, Y. Van Rompaey, and A. Persoons, Phys. Rev. Lett. **77**, 1456 (1996).

[45] S. Chen, B. Reineke, G. Li, T. Zentgraf, and S. Zhang, Nano Lett. **19**, 6278 (2019).

[46] B. M. Maoz, A. Ben Moshe, D. Vestler, O. Bar-Elli, and G. Markovich, Nano Lett. **12**, 2357 (2012).

[47] E. Plum, X.-X. Liu, V. A. Fedotov, Y. Chen, D. P. Tsai, and N. I. Zheludev, Phys. Rev. Lett. **102**, 113902 (2009).

[48] B. Gompf, J. Braun, T. Weiss, H. Giessen, M. Dressel, and U. Hübner, Phys. Rev. Lett. **106**, 185501 (2011).

[49] S. N. Volkov, K. Dolgaleva, R. W. Boyd, K. Jefimovs, J. Turunen, Y. Svirko, B. K. Canfield, and M. Kauranen, Phys. Rev. A **79**, 043819 (2009).

[50] M. Moocarme, N. V. Proscia, and L. T. Vuong, Sci. Rep. **7**, 40718 (2017).

[51] X. Zambrana-Puyalto, X. Vidal, and G. Molina-Terriza, Nat. Commun. **5**, 4922 (2014).

[52] D. Pan, H. Xu, and F. J. García de Abajo, Phys. Rev. Lett. **123**, 066803 (2019).

[53] S. Zu, T. Han, M. Jiang, F. Lin, X. Zhu, and Z. Fang, ACS Nano **12**, 3908 (2018).

[54] Z. Li, L. Kang, R. W. Lord, K. Park, A. Gillman, R. A. Vaia, R. E. Schaak, D. H. Werner, and K. L. Knappenberger, ACS Nanosci. Au **2**, 32 (2022).

[55] M. Ilchen, N. Douguet, T. Mazza, A. J. Rafipoor, C. Callegari, P. Finetti, O. Plekan, K. C. Prince, A. Demidovich, C. Grazioli, L. Avaldi, P. Bolognesi, M. Coreno, M. Di Fraia, M. Devetta, Y. Ovcharenko, S. Düsterer, K. Ueda, K. Bartschat, A. N. Grum-Grzhimailo *et al.*, Phys. Rev. Lett. **118**, 013002 (2017).

[56] K. Frizyuk, E. Melik-Gaykazyan, J.-H. Choi, M. I. Petrov, H.-G. Park, and Y. Kivshar, Nano Lett. **21**, 4381 (2021).

[57] J. García-Guirado, M. Svedendahl, J. Puigdollers, and R. Quidant, Nano Lett. **20**, 585 (2020).

[58] T. Kim and Q.-H. Park, Nanophotonics **11**, 1897 (2022).

[59] K. M. Czajkowski and T. J. Antosiewicz, Nanophotonics **11**, 4287 (2022).

[60] S. Both, M. Schäferling, F. Sterl, E. A. Muljarov, H. Giessen, and T. Weiss, ACS Nano **16**, 2822 (2022).

[61] K. Yao and Y. Liu, Nanoscale **10**, 8779 (2018).

[62] G. Rui, S. Zou, B. Gu, and Y. Cui, J. Phys. Chem. C **126**, 2199 (2022).

[63] R. Boyd, *Nonlinear Optics* (Academic, Cambridge, MA, 2002).

[64] M. Bertolotti, A. Belardini, A. Benedetti, and C. Sibilia, J. Opt. Soc. Am. B **32**, 1287 (2015).

[65] S. P. Rodrigues, S. Lan, L. Kang, Y. Cui, and W. Cai, Adv. Mater. **26**, 6157 (2014).

[66] J. D. Byers, H. I. Yee, T. Petralli-Mallow, and J. M. Hicks, Phys. Rev. B **49**, 14643 (1994).

[67] A. Nikolaeva, Tensor-rotation, 2022, https://github.com/kuyzirf/Tensor-rotation.

[68] See Supplemental Material at http://link.aps.org/supplemental/10.1103/PhysRevB.107.L041405 for a detailed theoretical description that shows how the main formula is obtained, numerical modeling, and the MATLAB code to obtain the tensor for a rotated lattice. We also show the nonlinear polarization for several cases, and the modeling results.

[69] S. Gladyshev, K. Frizyuk, and A. Bogdanov, Phys. Rev. B **102**, 075103 (2020).

[70] K. Frizyuk, I. Volkovskaya, D. Smirnova, A. Poddubny, and M. Petrov, Phys. Rev. B **99**, 075425 (2019).

[71] K. Frizyuk, J. Opt. Soc. Am. B **36**, F32 (2019).

[72] C. Gigli, T. Wu, G. Marino, A. Borne, G. Leo, and P. Lalanne, ACS Photonics **7**, 1197 (2020).

[73] P. Lalanne, W. Yan, K. Vynck, C. Sauvan, and J.-P. Hugonin, Laser Photonics Rev. **12**, 1700113 (2018).

[74] S. Cabuk, Open Phys. **10**, 239 (2012).

[75] Z. Xiong, Z. Xiong, Q. Yang, Q. Yang, W. Chen, Z. Wang, J. Xu, J. Xu, J. Xu, W. Liu, Y. Chen, Y. Chen, and Y. Chen, Opt. Express **28**, 3073 (2020).

[76] M. B. Doost, W. Langbein, and E. A. Muljarov, Phys. Rev. A **90**, 013834 (2014).

[77] I. Deriy, I. Toftul, M. Petrov, and A. Bogdanov, Phys. Rev. Lett. **128**, 084301 (2022).

[78] I. Toftul, G. Fedorovich, D. Kislov, K. Frizyuk, K. Koshelev, Y. Kivshar, and M. Petrov, arXiv:2210.04021.

[79] L. Carletti, L. Carletti, L. Carletti, C. Li, C. Li, J. Sautter, I. Staude, C. De Angelis, T. Li, and D. N. Neshev, Opt. Express **27**, 33391 (2019).

[80] M. Timofeeva, L. Lang, F. Timpu, C. Renaut, A. Bouravleuv, I. Shtrom, G. Cirlin, and R. Grange, Nano Lett. **18**, 3695 (2018).